

引用格式: MA Chaofeng, JIANG Qi, WU Ying, et al. Underwater Frequency Modulated Continuous Wave Laser Ranging Based on Blue External Cavity Diode Laser[J]. Acta Photonica Sinica, 2023, 52(6):0614001

马超峰,姜琦,吴映,等.基于蓝光外腔半导体激光器的水下调频连续波激光测距[J].光子学报,2023,52(6):0614001

基于蓝光外腔半导体激光器的水下调频连续波激光测距

马超峰^{1,2},姜琦^{1,2},吴映²,梁伟^{1,2,3}

(1 中国科学技术大学 纳米技术与纳米仿生学院,合肥 230026)

(2 中国科学院苏州纳米技术与纳米仿生研究所,苏州 215123)

(3 安徽大学 光电信息获取与控制教育部重点实验室,合肥 230601)

摘要:采用商用 405 nm FP 蓝光激光二极管,外加反射镜组成窄线宽外腔半导体激光器,在 1 kHz 调制周期下获得了无跳模连续调频范围 1.5 GHz,相干长度大于 10 m 的激光输出。注入电流直接调制进行扫频,搭建空间光干涉仪组成调频连续波激光测距系统,采用 10 m 延时光纤辅助干涉仪对拍频信号进行重采样,以降低调制非线性对测距精度的影响。在水箱中模拟海水的衰减系数,在 9.5 mW 的探测信号功率下验证了 5 m 距离的探测,最大测量偏差 0.051 m。

关键词:水下测距;调频连续波;蓝光激光;重采样;窄线宽

中图分类号:TN247

文献标识码:A

doi:10.3788/gzxb20235206.0614001

0 引言

近年来,自主式水下机器人(Autonomous Underwater Vehicle, AUV)已成为海洋探索及水下作业的重要手段,一种低功耗、轻量化水下激光测距系统对小型 AUV 环境感知有着重要的意义^[1-4]。现有的水下激光雷达大多是基于脉冲飞行时间(Time Of Flight, TOF)^[5-6]进行测距,典型的脉冲长度 12 ns,峰值功率约为 333 kW,探测距离约 26 m,测距精度小于 0.6 m。但是其体积庞大,功耗较高,通常使用飞机、舰船等作为负载平台^[7-8],不适合 AUV 等小型平台的应用。此外,基于 TOF 的激光雷达之间也会存在干扰。后向散射也是水下脉冲激光雷达面临的一个巨大挑战^[9-10],后向散射降低了测距的对比度和分辨率,强烈的后向散射会极大的限制探测系统的动态范围,甚至淹没目标信号导致检测到虚假的目标^[9]。常用的抑制水下后向散射的方法有距离选通技术^[11]和同步扫描技术^[12],但是上述两种方法存在一定的距离死区,且测量速度非常慢。目前,针对自动驾驶应用的近红外波长激光调频连续波(Frequency Modulated Continuous Wave, FMCW)激光雷达^[13-15]已日渐成熟,然而,至今还鲜有关于水下调频连续波激光雷达的研究报道。水下调频连续波激光雷达具有比 TOF 雷达更大的动态范围,可以输出与距离成比例的连续的频谱信号。FMCW 激光雷达的距离分辨率只与激光器的调频范围有关,因此可以用较低带宽的探测器达到较高的距离分辨率^[14]。此外,由于相干探测的本振光对输出的放大作用,相干探测的灵敏度非常高,因此 FMCW 激光雷达对激光器输出功率要求相对较低,可以使用体积小功耗低的半导体激光器实现,非常适合对尺寸、重量、功耗等要求非常高的应用。

单纵模窄线宽可调频激光器是调频连续波激光雷达的前提,由于水对光的吸收损耗^[16-17]会导致信号衰减从而缩短探测距离,因此需选用位于海水“透射窗口”^[1]、衰减系数较小的蓝绿激光。由于蓝光波长较短,

基金项目:国家自然科学基金(No. 62075233),中国科学院稳定支持基础研究领域青年团队计划(No. YSBR-69),光电信息获取与控制教育部重点实验室(安徽大学)开放基金

第一作者:马超峰, cfma2021@sinano.ac.cn

通讯作者:梁伟, wliang2019@sinano.ac.cn

收稿日期:2023-01-01; **录用日期:**2023-02-17

<http://www.photon.ac.cn>

所需的分布反馈周期很小,近红外波长常见的DFB单频窄线宽激光器所需的半导体刻蚀工艺在蓝绿波长极难实现,目前还没有商业化的蓝绿波长DFB激光产品。有研究人员尝试在DFB结构中埋入相移光栅,实现了波长450 nm的单模激光输出^[18]。该激光器线宽约3 GHz,相干长度不足0.1 m,无法满足数米以上的FMCW测距需求。有学者利用钛宝石激光器腔内倍频技术实现455.5 nm激光输出,线宽1.8 MHz,连续扫频范围3.4 GHz^[19]。该激光器虽然可以满足FMCW水下测距的性能要求,但是其结构复杂,体积庞大且稳定性较低。本文采用商用405 nm蓝光FP激光二极管组成外腔半导体激光器(External-Cavity Diode Laser, ECDL),相干长度大于10 m,在1 kHz扫频周期下可实现无跳模连续扫频范围1.5 GHz。使用该ECDL激光,搭建了调频连续波测距装置,进行水下测距实验,测距频率1 kHz,平均测量偏差小于0.051 m。

1 基本原理

1.1 调频连续波测距原理

调频连续波激光测距的基本原理如图1(a)所示,信号发生器产生三角波调制信号,通过改变注入电流对激光进行频率调制。光源发出的调制激光经过分束器(Beam Splitter, BS)分为两部分,一部分作为探测信号发射到目标物体上,另一部分作为本振光与反射回来的光发生干涉,混频后得到两信号的拍频信号,此拍频信号的频率包含着目标距离和速度等信息。因此,将拍频信号进行快速傅里叶变换(Fast Fourier Transform, FFT)等相关处理,即可计算出目标距离等信息^[13]。

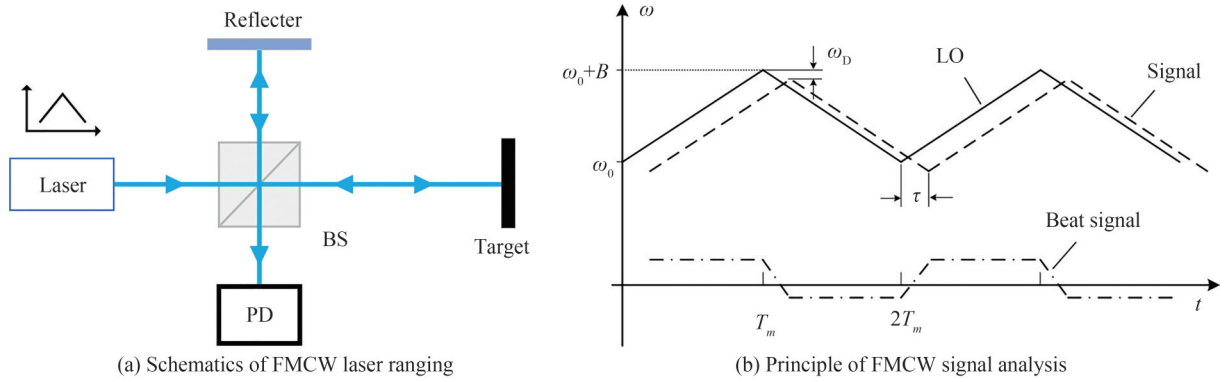


图1 调频连续波激光测距原理示意图

Fig.1 Schematic diagram and principle of FMCW signal analysis

图1(b)中实线为本振光信号的角频率波形,虚线为回波信号的角频率波形,点划线为混频生成的拍频信号的角频率波形。采用三角波调制信号,其周期为 $2T_m$,在上升阶段,本振光信号的角频率为^[13]

$$\omega_1(t) = \omega_0 + 2\pi \frac{B}{T_m} t = \omega_0 + \alpha t \quad (1)$$

式中, ω_0 为起始频率, B 为三角波的调频范围, α 为三角波调制斜率。当两束光发生干涉时,得到的混频信号强度可表示为^[13]

$$I(\tau, t) = I_0 \left[1 + V \cos \left(\alpha \tau t + \omega_0 \tau - \frac{\alpha \tau^2}{2} \right) \right] \quad (2)$$

式中, I_0 和 V 分别是拍频信号的平均强度和对比度。 τ 是调频光从BS输出到待测点再返回的传播时间,为

$$\tau = \frac{2nl}{c} \quad (3)$$

式中, n 为传播介质的折射率, c 为自由空间中的光速。从而可以得到拍频信号的角频率为

$$\omega_b = \alpha \tau \quad (4)$$

在频率调制的上升段和下降段,其拍频频率绝对值是相等的且都为 ω_b ,因此可以得到目标距离为^[14]

$$l = \frac{T_m c}{2nB} \omega_b \quad (5)$$

FMCW激光测距的距离分辨率为^[14]

$$\Delta l = \frac{c}{2nB} \quad (6)$$

由式(6)可知,在调频范围 B 和周期 T_m 一定的条件下,拍频信号的频率与距离成正比,测量拍频信号的频率即可计算出距离 l ,同时从式(6)可以看出FMCW激光测距的距离分辨率只取决于调频范围,因此理论上,提高激光光源的调频范围 B 可以提高理论测距分辨率。

1.2 重采样

FMCW激光雷达测距对激光的调频线性度有着很高的要求。在实际应用中,激光器的频率通常并不是随调制信号线性变化的^[20],直接测量拍频信号的频率也不是恒定值,这会导致FFT后的信号频谱展宽,降低测距的信噪比以及测量精度。因此需要解决调制非线性带来的影响,并调控中心波长使线性扫频范围尽可能宽。

这个问题可以通过在频域对干涉信号瞬时等光频间隔采样^[21],而非等时间间隔采样来避免。通常使用方法是通过对一个辅助的马赫-曾德尔干涉仪监控频率随时间的变化,其延时光纤的长度必须保持不变,并且延迟光程差至少大于主干涉仪光程差的2倍。两个干涉仪拍频信号由ADC同步采样,将辅助干涉仪信号的每个峰值和谷底的时间点作为触发,对主干涉仪的拍频信号进行重新采样。由于调制非线性对两个干涉仪的影响是相同的,重采样的信号中不包含非线性的相位噪声,因此可以很大程度上消除非线性频率扫描引起的误差,文献[21]对重采样的原理及对分辨率的影响做出了详细分析。

提取辅助干涉仪拍频信号的峰值位置点,其光频间隔为 $\Delta\omega = \pi/\tau_r$,其中 τ_r 为辅助干涉仪的光纤延时。由于 τ_r 为恒定值,峰值点之间的光频间隔不变。重采样得到的拍频信号可表示为^[21]

$$I(\tau_m, k) = I_{m0} \left[1 + V_m \cos \left(\frac{\pi\tau_m}{\tau_r} k + \omega_0\tau_m \right) \right] \quad (k=0,1,2,\dots) \quad (7)$$

式中, I_{m0} 、 V_m 分别为主测量干涉仪拍频信号的平均强度和对比度, τ_m 为主测量干涉仪的传播时间。实际情况中式(2)的 α 包含随时间变化的非线性项,导致拍频信号频谱展宽,而重采样后的拍频信号为理想的余弦采样函数,其中不包含调制非线性的部分,因此重采样技术可以优化干涉信号的频谱展宽,提高测距精度。对其进行FFT运算获取其频谱,代入式(3)、(4)可得待测目标距离为

$$l = \frac{n_1 LP}{n_2 N} \quad (8)$$

其中, n_1 为延时光纤折射率, n_2 为传播介质折射率, L 为延时光纤长度, N 为采样点总数, P 为频谱峰值点位置。

2 实验装置

2.1 蓝光单模可调光源

调频连续波激光雷达的精度、分辨率和测量范围等性能与光源的参数密切相关。根据FMCW激光测距原理,激光器的相干长度必须大于测距范围的两倍^[22];并且激光器的调频范围越大,距离分辨率越小。单纵模无跳模窄线宽激光输出是实现调频连续波测距的前提。

如图2所示,本文采用一种最为简单的外腔半导体激光结构^[24-25],该外腔半导体激光器由半导体激光、准直透镜、30%反射镜以及隔离器组成,相较Ti宝石激光器^[19]具有结构简单、体积小等优点,其中光源使用中心波长405 nm的商用FP多纵模半导体激光二极管,纵模间隔约50 pm,发光功率可达20 mW以上。激光

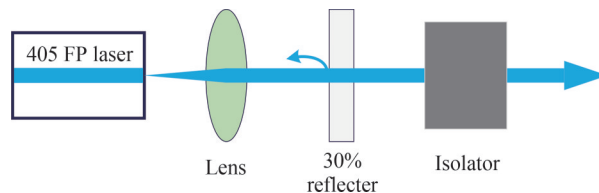


图2 蓝光外腔半导体激光器
Fig.2 Blue light external cavity semiconductor laser

二极管输出的光束经准直透镜发射到反射镜上,30%的反射光沿入射光路反馈回激光二极管。激光二极管原有的多纵模,在外腔反馈时具有不同的反馈相位,从而形成不同的相干反馈增益并进而产生单频输出,此外由于外腔显著增加了激光的等效腔长和品质因子,激光的线宽也得到了压窄。实验中发现,要获得单模激光输出需要选取合适的反射率,反射率太低会导致反馈光太弱,无法形成有效的外腔反馈选模;反射率太高会降低激光器的出光效率,同时对激光二极管也会有一定的损害。另外,激光的线宽和调频范围与外腔的腔长有关,因此需要合理地调节反射镜的位置以满足线宽与调频范围需求^[25]。

图3所示为固定注入电流下,有无外腔反馈的激光光谱及扫频干涉信号对比,图3(a)中蓝色线为未加反射镜的FP光源输出光谱,当调节30%反射镜垂直于出光光路形成外腔反馈后,由于外腔反馈对激光器具有选模和压缩线宽的作用^[24],并且通过位移反射镜选取合适的反馈相位,可形成如橙色线所示的单纵模单频激光输出,中心波长408 nm。本实验采用10 m延时光纤搭建光纤干涉仪,图3(b)展示了对激光注入电流进行三角波调制时,在加反射镜形成外腔前后的干涉信号对比。其中蓝色线为未加反射镜的FP光源调频输出的干涉信号,由于此时的输出为多模激光,激光总有效相干长度较短无法形成高对比度的干涉信号。橙色线为有反射镜时的激光调频干涉信号,可以看出单模激光可以形成高对比度的干涉现象,说明外腔半导体激光器的相干长度远大于10 m光纤光程,对应的激光线宽约为或优于MHz量级^[22],因此其测距性能优于已报道的DFB激光器^[18]。

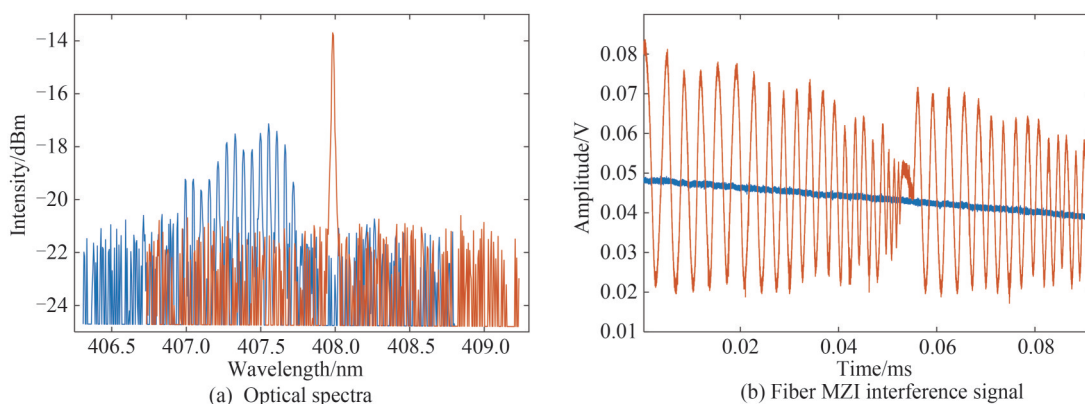


图3 蓝光FP激光在有和无外腔反馈时的光谱和干涉仪信号对比

Fig.3 Comparison of the optical spectrum and the interference signal of the diode laser with and without external feedback

2.2 测距装置

本文所设计的基于调频连续波激光测距的系统框架如图4所示。实验系统主要包括:光学测量系统、数据处理电路、水下测试环境。其中光学系统部分由单模可调谐的激光光源、用于测距的空间光干涉仪以及用于重采样的辅助光纤干涉仪组成。

实验光学测量系统如图4(a)所示,通过信号发生器产生1 kHz的三角波调制信号对光源的注入电流进行调制,使用辅助干涉仪测量激光无跳模连续调频范围约1.5 GHz。输出的激光经过BS分成两束,90%进入测量干涉系统,另一路进入辅助干涉系统。测量干涉仪系统中,激光经过偏振分束器(Polarization Beam Splitter, PBS)分成96:4两路,4%一路发射到反射镜上作为干涉仪的本振光;96%一路经过自由空间发射到被测目标上,输出光功率9.5 mW,假设目标不改变入射光偏振方向,本振光路和探测光路的1/4波片可使得反射的本振和探测光信号在PBS1分别透过和反射形成合束。本振光和信号光经过光轴夹角22.5°的1/2波片及PBS2后分别分为偏振正交的两束光,相位相差180°,分别进入光电探测器(Photodetector, PD)形成平衡探测^[23]。由于PD1和PD2的信号相位相差180°,通过平衡探测器中的差分放大电路后共模部分抑制相消,差模部分放大,因此采用平衡探测可有效抑制拍频信号中的直流分量提取交流分量,从而将干涉信号放大。辅助干涉仪系统中,激光经50:50光纤耦合器(Optical Coupler, OC)分为两束,其中一束经过10 m延时光纤后与另一束混频,产生的混频信号由光电探测器输出。数据处理电路部分主要以FPGA作为控制,通过ADC将测量干涉系统中的探测信号与辅助干涉系统中的探测信号同步采集,通过以太网发送到上位机进行信号的重采样与傅里叶频谱分析。

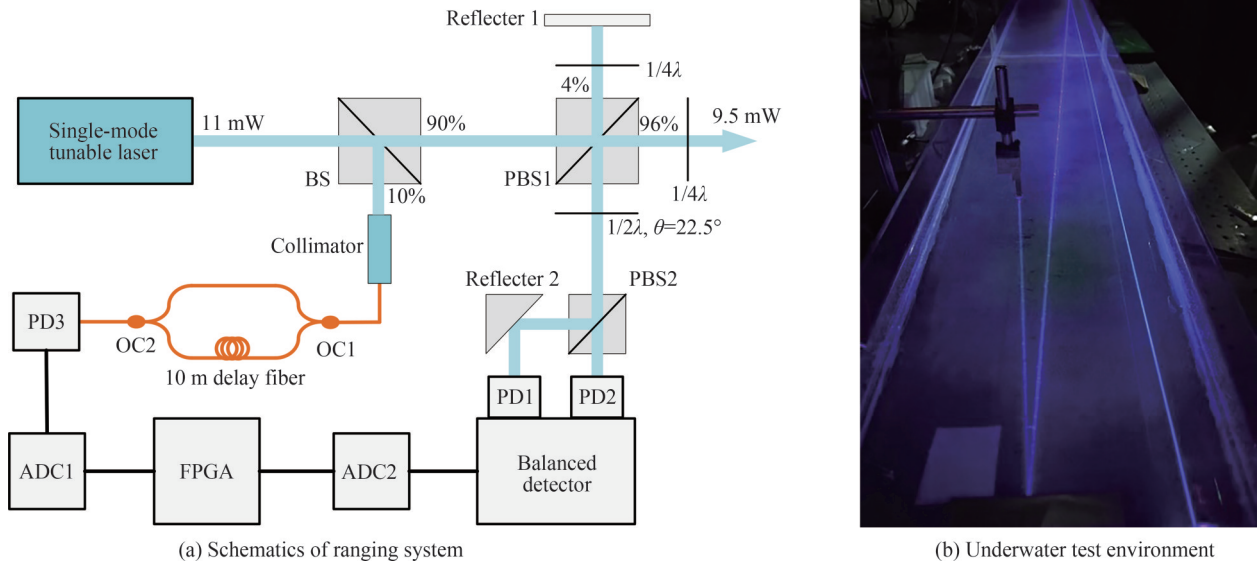


图4 测距系统原理图
Fig.4 Schematic diagram of ranging system

实验水下测试环境如图4(b)所示,通过在2 m长水箱中添加 $Mg(OH)_2$ 粉末调节水的混浊度,得到了衰减系数 1.2 m^{-1} [17]的水下测试环境,水的折射率约为1.33[3]。测距系统为同轴系统,水箱入光口选用直径10 mm透射率99%的光学窗口平面,水箱两端放置反射镜通过多次反射延长实验测试距离,在不同位置放置反射率95%的反射镜作为探测目标物,模拟海水环境进行水下测距。

3 实验结果与分析

实验中,先直接对探测到的拍频电压信号进行傅里叶变换,以对数坐标展示其频谱功率的相对大小,由于目标距离与干涉信号的频率成正比,可通过式(5)将FFT频谱转换为距离坐标,直观体现拍频信号与测量距离的分布关系,得到的频谱如图5(a)所示。由于激光器频率调制非线性的影响,可以看出拍频信号频谱发生了严重展宽,此时目标距离的测量精度非常差[21],信噪比也下降。图5(b)展示了采用辅助干涉仪对拍频信号等频率间隔重采样后的傅里叶频谱,可以明显看出拍频信号的展宽得到了很好的修正,信噪比也有了显著提高,可以更精确地检测出频谱峰值的频率,从而准确获得目标物体的距离信息。实验验证了等频率间隔重采样对调制非线性影响的抑制具有显著的效果。

利用重采样技术对不同位置目标进行测距实验,将目标物在水下逐次移动0.5 m进行距离探测。图6所示为不同位置探测目标的干涉信号傅里叶频谱,从图中可以看出在不同的探测距离下回波信号均有大于10 dB的信噪比。随着探测距离的增加,干涉信号的强度和信噪比逐渐降低,测距误差也会随之增加,系统

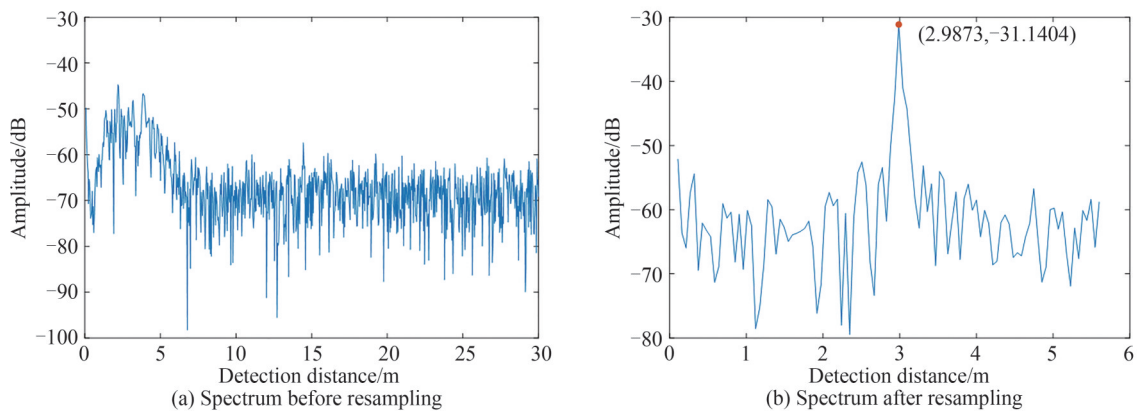


图5 重采样前后FFT频谱对比
Fig.5 FFT spectrum comparison before and after resampling

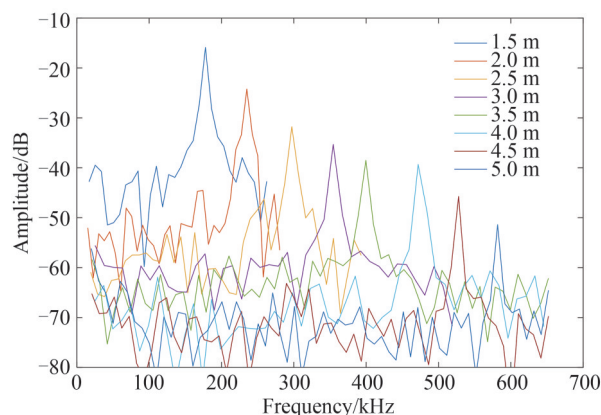


图6 FMCW测距结果
Fig.6 FMCW ranging results

的最大可验证探测距离约为5 m,此时拍频信号频率约为580 kHz,信噪比约为15 dB。

实验在绝对距离1.5 m~5 m的范围内逐点测量5次取平均值,得到的测量距离分别为1.524 m、2.009 m、2.551 m、3.024 m、3.469 m、4.039 m、4.550 m和5.023 m。从图7中可以看出目标测量距离与实际距离呈良好的线性关系,在不同的测量距离下最大拟合偏差为0.051 m。

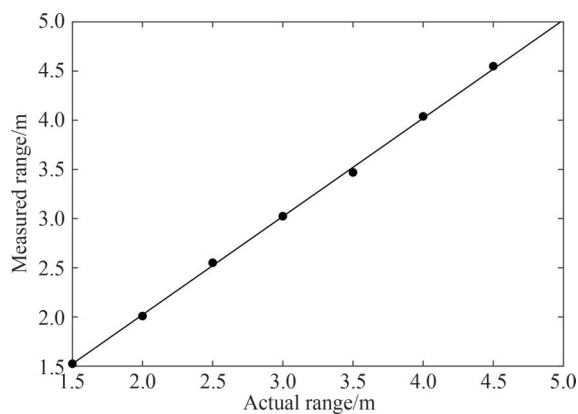


图7 实际距离与测量距离关系
Fig.7 Relationship between actual distance and measured distance

理论上FMCW激光测距的距离分辨率只取决于调频范围,从式(6)可计算得到距离分辨率为0.075 m。实际测量中,重采样过程会减少采样点数,从而降低FFT频谱分析的精度;同时待测目标物体的位置由钢卷尺测量得到,也会引入<1 cm的测量误差。图8展示了3 m距离下的十组测量结果,其中最大测量误差为

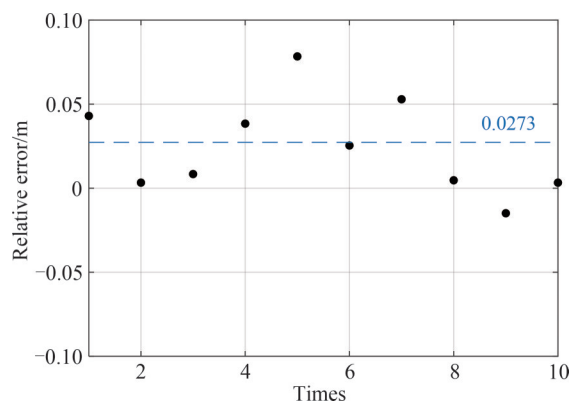


图8 距离测量误差
Fig.8 Distance measurement error

0.08 m,计算得到平均误差为0.027 m,均低于FMCW理论距离分辨率。

4 结论

本文提出并实现了基于调频连续波原理的水下蓝光激光测距。采用自行设计组装的可调谐外腔半导体激光器,实现了波长408 nm无跳模连续扫频范围1.5 GHz,相干长度大于10 m光纤的蓝光激光输出。相较于其他结构外腔蓝光激光^[24-25]具有结构简单、体积小等优点。实验搭建调频连续波激光测距系统,在 1.2 m^{-1} 衰减系数的水下对从1.5到5米间的反射目标进行了测距实验,最大测量偏差0.051 m,测量信号信噪比 $>10\text{ dB}$ 。实验证明水下蓝光调频连续波激光测距系统符合理论预期的高分辨率的测距性能,并具有低功率、体积小、成本低等优点。为水下作业的小型无人机平台提供一种低功耗、轻量化的环境感知测距方案。

参考文献

- [1] 李哲,邓甲昊,周卫平.水下激光探测技术及其进展[J].舰船电子工程,2008,28(12):8-11,48.
- [2] COCHENOUR B, MULLEN L, MUTH J. Modulated pulse laser with pseudorandom coding capabilities for underwater ranging, detection, and imaging[J]. Applied Optics, 2011,50(33):6168-6178.
- [3] ZHANG Mingtao, ZHANG Jianzhong, ZHANG Jianguo, et al. Chaotic modulation lidar for underwater ranging[J]. Laser & Optoelectronics Progress, 2016, 53(5): 051402.
张明涛,张建忠,张建国,等.面向水下测距的混沌调制激光雷达[J].激光与光电子学进展,2016,53(5):051402.
- [4] SUN Youchun, PANG Yajun, BAI Zhenxu. Application technology of laser triangulation[J]. Laser Journal, 2021,42(4):1-8.
孙有春,庞亚军,白振旭,等.激光三角测量法应用技术[J].激光杂志,2021,42(4):1-8.
- [5] JIN W, CAO F, WANG X, et al. Range-gated underwater laser imaging system based on intensified gate imaging technology[C]. Applied Optics and Photonics China, 2008.
- [6] CHENG Z, YANG K, HAN J, et al. Improved time-of-flight range acquisition technique in underwater lidar experiments[J]. Applied Optics, 2015,54(18):5715-5725.
- [7] LIU H, CHEN P, MAO Z, et al. Subsurface plankton layers observed from airborne lidar in Sanya Bay, South China Sea[J]. Optics Express, 2018,26(22):29134-29147.
- [8] CHEN P, JAMET C, ZHANG Z, et al. Vertical distribution of subsurface phytoplankton layer in South China Sea using airborne lidar[J]. Remote Sensing of Environment, 2021,263:112567.
- [9] LIN X, YANG S, LIAO Y. Backward scattering suppression in an underwater LiDAR signal processing based on CEEMDAN-fast ICA algorithm[J]. Optics Express, 2022,30(13):23270-23283.
- [10] SHEN Zhenmin, SHANG Weidong, WANG Bingjie, et al. Lidar with high scattering ratio suppression for underwater detection[J]. Acat Photoncia Sinica, 2020, 49(6):0601001.
沈振民,尚卫东,王冰洁,等.高散射抑制比激光雷达水下探测技术探析[J].光子学报,2020,49(6):0601001.
- [11] ALEM N, PELLEN F, LE BRUN G, et al. Extra-cavity radiofrequency modulator for a lidar radar designed for underwater target detection[J]. Applied Optics, 2017,56(26):7367-7372.
- [12] JAFFE J S. Performance bounds on synchronous laser line scan systems[J]. Optics Express, 2005,13(3):738-748.
- [13] ZHENG J. Analysis of optical frequency-modulated continuous-wave interference[J]. Applied Optics, 2004, 43(21):4189-4198.
- [14] MENG Xiangsong, ZHANG Fumin, QU Xinghua. High precision and fast method for absolute distance measurement based on resampling technique used in FM continuous wave laser ranging[J]. Acta Physica Sinica, 2015, 64(23): 230601.
孟祥松,张福民,曲兴华.基于重采样技术的调频连续波激光绝对测距高精度及快速测量方法研究[J].物理学报,2015,64(23):230601.
- [15] ROOS P A, REIBEL R R, BERG T, et al. Ultrabroadband optical chirp linearization for precision metrology applications[J]. Optics Letters, 2009,34(23):3692-3694.
- [16] ILLIG D W, JEMISON W D, LEE R W, et al. Optical ranging techniques in turbid waters: sensing technologies+ applications[C]. SPIE, 2014.
- [17] LI Kun, YANG Suhui, LIAO Yingqi, et al. Underwater ranging with intensity modulated 532 nm laser source[J]. Acta Physica Sinica, 2021, 70(8): 084203.
李坤,杨苏辉,廖英琦,等.强度调制532 nm激光水下测距[J].物理学报,2021,70(8):084203.
- [18] ZHANG H, COHEN D A, CHAN P, et al. High performance of a semipolar InGaN laser with a phase-shifted embedded hydrogen silsesquioxane (HSQ) grating[J]. Optics Letters, 2020,45(20):5844-5847.
- [19] LI F, LI H, LU H. Realization of a tunable 455.5-nm laser with low intensity noise by intracavity frequency-doubled Ti:

- sapphire laser[J]. IEEE Journal of Quantum Electronics, 2016,52(2):1-6.
- [20] ZHANG X, POULS J, WU M C. Laser frequency sweep linearization by iterative learning pre-distortion for FMCW LiDAR[J]. Optics Express, 2019,27(7):9965-9974.
- [21] BAO Weizheng, ZHANG Fumin, QU Xinghua. Laser ranging method of frequency modulation interference based on equal optical frequency subdivision resampling[J]. Laser Technology, 2020, 44(1):1-6.
包为政, 张福民, 曲兴华. 基于等光频细分重采样的调频干涉测距方法[J]. 激光技术, 2020,44(1):1-6.
- [22] 祝建芳. 电流调谐DFB激光器调频线性化研究[D]. 重庆:重庆理工大学, 2020.
- [23] 李玉. 基于平衡探测器的光外差探测系统研究[D]. 长沙:国防科学技术大学, 2015.
- [24] HUA Jinping, JIANG Yi. Recent progresses of tunable external cavity diode laser[J]. Semiconductor Optoelectronics, 2021,42(1):11-19, 56.
花金平, 江毅. 可调谐外腔半导体激光器研究进展[J]. 半导体光电, 2021,42(1):11-19, 56.
- [25] 柴燕杰, 吴群, 张汉一, 等. 窄线宽外腔半导体激光器[J]. 激光与红外, 1988, (10):7-9.
- [26] ZHU Y, ZENG S, ZHAO X, et al. Narrow-linewidth, tunable external cavity diode lasers through hybrid integration of quantum-well/quantum-dot SOAs with Si_3N_4 microresonators [C]. 2018 Conference on Lasers and Electro-Optics (CLEO), 2018:1-2.

Underwater Frequency Modulated Continuous Wave Laser Ranging Based on Blue External Cavity Diode Laser

MA Chaofeng^{1,2}, JIANG Qi^{1,2}, WU Ying², LIANG Wei^{1,2,3}

(1 School of Nano-Tech and Nano-Bionics, University of Science and Technology of China, Hefei 230026, China)

(2 Suzhou Institute of Nano-Tech and Nano-Bionics, Chinese Academy of Sciences, Suzhou 215123, China)

(3 Key Laboratory of Opto-Electronic Information Acquisition and Manipulation, Ministry of Education, Anhui University, Hefei 230601, China)

Abstract: Underwater lidar technology has become an important tool for ocean exploration and underwater operations. So far, all of the reported underwater lidars are based on the pulsed Time-Of-Flight (TOF) method for ranging, which is characterized by high pulse peak power and relatively long detection distance. However, TOF lidar is large in size, high in power consumption, and small in dynamic range, and there will be interference between different TOF lidars. Hence they are not suitable for compact platforms such as Autonomous Underwater Vehicles (AUV) swarms. In addition, back scattering presents a great challenge to underwater pulsed lidar, which limits the sensitivity and dynamic range of the detector. Strong back scattering of suspended solids in water can completely submerge the real signal, leading to false target detection. Underwater Frequency Modulated Continuous Wave (FMCW) lidar has a greater dynamic range than TOF radar and can output a continuous spectral signal proportional to distance. Because the signal of the coherent detection is amplified by the local oscillator, FMCW lidar requires low laser output power and can be realized with low power diode laser, which can significantly reduce the size, weight and power of the lidar system. So far most reported studies on FMCW lidar are concentrated on near-infrared wavelength such as 1 μm , 1.55 μm . However, there have been no reports of underwater FMCW lidar using blue or green lasers so far.

The implementation of FMCW lidar is faced with two challenges, one is to obtain a single-mode tunable narrow linewidth laser, the other is to eliminate the nonlinear effect of laser frequency modulation. Because the light absorption loss of water will lead to the signal attenuation and shorten the detection distance, it is necessary to select the blue-green laser located in the seawater "transmission window" with a small attenuation coefficient. A commercial 405 nm Blue FP laser diode and a 30% reflector are used to construct an External Cavity Diode Laser (ECDL). The blue ECDL exhibits a coherence much longer than 10 meters in fiber, and a continuous frequency sweep range of 1.5 GHz by direct modulation of the injection current. Modulation nonlinearity of the FMCW laser can broaden the FFT spectrum of the measured signal and reduce the ranging accuracy. To overcome this problem, an FMCW ranging method based on equal optical frequency resampling is adopted. The system consists of both a fiber interferometer and a free space interferometer. The optical fiber interferometer uses 10 m delay optical fiber to monitor the frequency

change with time, and the free space interferometer is used to obtain the beat frequency signal containing the distance information of the target to be measured. Theoretical analysis and experimental verification were carried out. The underwater ranging was conducted by adding $Mg(OH)_2$ powder in the water tank to adjust the attenuation coefficient to simulate the seawater environment. An FMCW laser ranging system with dual interferometers is built, and the extremum point of the beat signal of the fiber optic interferometer is extracted to sample the beat signal of the free space Interferometer. It is verified that the beat signal spectrum broadening problem due to the laser's frequency modulation nonlinearity is well corrected. Using the resampling method, the distance is measured at eight equally spaced positions, and a reflector is placed at these positions in turn as the detection target. The results show that the measurement range of the target is linear with the actual range, and a detection range of 5 meters is realized with only 9.5 mW laser output power, and the maximum error is 0.051 m. In order to obtain the measurement error of the FMCW ranging system, ten groups of data are measured at the same position. Through calculation, the average measurement error of the ranging system is 0.027 m. Our work demonstrates that a low power commercial blue laser diode can be used to construct a single frequency ECDL laser, and it can be directly frequency modulated to perform accurate underwater FMCW laser ranging. This lidar architecture characterizes by small size, low power and weight, which promises an effective laser ranging sensor for compact AUV swarm.

Key words: Underwater ranging; Underwater frequency modulated continuous wave; Blue laser; Resampling; Narrow linewidth

OCIS Codes: 140.3600; 140.5960; 280.3400; 280.3420; 280.3640